DOI:10.1190/FWI2017-028

LSRTM enhanced with inverse scattering imaging condition

Xiuzheng Fang[1], Di Wu[1], Fenglin Niu[1]
[1]China University of Petroleum-Beijing

Summary

The least-squares reverse-time migration (LSRTM) has the advantages of high resolution, amplitude equalization and amplitude preservation, and can be used for effective imaging of complex geological structures. However, the gradient of the objective function calculated by the adjoint-state method may suffer from low frequency artifacts which will slow down the convergence and the reflectivity image cannot be effectively updated during the iterations. In this paper, we propose a linear Born inverse scattering imaging operator to efficiently update the gradient with respect to the model parameters, the numerical results show that the linear Born inverse scattering imaging condition can update the gradient of the objective function efficiently and improve the imaging quality effectively.

Introduction

Reverse-time migration (RTM) is often used to enhance the image quality in areas with complex subsurface structures and strong velocity contrasts whilst other migration methods may become inadequate to give high quality images. The use of the two-way wave equation for seismic imaging was initially proposed by several authors in the early 1980s (Baysal et al., 1983). On the one hand, RTM can provide high quality images of steep-dip reflectors and improve complex areas images as two-way wave equation is used. On the other hand due to the essence of the two-way wave equation, strong velocity gradients or reflecting interfaces in the migration velocity model will lead to backscattering of the energy of forward (backward)-propagated source (receiver) wavefields. RTM with the conventional cross-correlation imaging condition, which is based on the imaging principle proposed by Clearbout (1971), suffers from low frequency artifacts that result from the backscattered energy of source and receiver wavefields crosscorrelated along the nonphysical wave paths. Several schemes have been proposed to deal with the low frequency noise issue. Baysal et al., (1984) introduced the nonreflecting wave equation by matching the impedance of the media to reduce reflections from material interfaces. Loewenthal, et al., (1987) suggested smoothing the velocity model to reduce the reflections. Fletcher et al., (2005) applied the directional damping factor to suppress backscattered energy. Yoon and Marfurt (2006) adopted the Poynting vector to eliminate the low frequency artifacts. Zhang and Sun (2009) propose to apply Laplace filter to attenuate the artifacts and improve the migration quality. Liu et al., (2011) proposed to separate upgoing and downgoing wavefields to eliminate such noise based on the Hilbert transform. Op't Root et al. (2012) introduced a linearized inverse scattering imaging condition to suppress the low-frequency imaging artifacts.

With increasing requirements for image accuracy and amplitude preserving in seismic exploration, it is necessary to improve conventional migration methods, which employ the conventional crosscorrelation imaging condition. Least-squares migration formulated as an inverse problem based on a least-squares function of the data residuals in the way of linear optimization and numerical iteration has shown its good performance on image accuracy, amplitude preserving and image resolution. The first implementation of the least-squares migration was the Kirchhoff migration (Nemeth et al., 1999). Recently, least-square migration has been implemented with reverse-time migration called least-squares RTM (LSRTM) (Dai et al., 2012; Yao et al.,2012, 2015, 2016). However, the gradient of the functional of LSRTM calculated by the adjoint-state method (the conventional cross-correlation imaging condition) suffer from low frequency artifacts which slow down the convergence during the iterations and the update of the gradient of the objective function is inefficient.

In this paper, we propose the linear Born inverse scattering imaging condition to update the gradient of the objective function during the iterations without any type of additional image filters. Result shows that it can suppress the low-frequency noise, accelerate the convergence and improve the imaging quality effectively.

Theory

According to scattering theory, single scattering approximation of acoustic wave equation based on Born approximation gives the single scattered wavefield $d(x_r;x_s,\omega)$, i.e., primary reflection, recorded at the receiver location from the source location defined as equation (1),

$$d(x_r;x_s,\omega)=\omega^2\int G_0(x_r;x,\omega)m(x)G_0(x;x_s,\omega)s(\omega)dx \quad (1)$$

where x_{r} is the receiver location and x_s is the source location. ω is the angular frequency. $G_0(x_r;x,\omega)$ and $G_0(x;x_s,\omega)$ are the Green's functions associated with the background velocity and projects a wavefront a positive distance from the source point x_s to some scattering point x and from the scattering point x to the receiver point as time increase respectively. $m(x)$ is the reflectivity model at the subsurface of the study area, defined as following,

DOI:10.1190/FWI2017-028

$$m(x) = \frac{\delta v(x)}{v_0(x)} \tag{2}$$

where $v_0(x)$ is the reference velocity, and $\delta v(x)$ is perturbation velocity. Since Born approximation only stands for a very small perturbation, it is required that the background velocity is relatively accurate.

For the sake of brevity, acoustic wave equation based on Born approximation can be called for state equations and the wavefield, p , satisfy the state equations defined with the mapping, F ,

$$F(p(m), m) = p(m) - Lm = 0 \tag{3}$$

Where $p(m)$ is the wavefield in the frequency domain, and $L = \omega^2 \int G_0(x; x', \omega) G_0(x'; x_s, \omega) s(\omega) dx'$ is the linearized Born modelling operator, which is also known as de-migration operator. F is also called the de-migration equation or forward equation. m is the model parameter.

To improve the image accuracy, resolution and amplitude-preserving, the least-squares error function can be minimized iteratively by taking the off-diagonal terms of the Hessian into account. Given synthetic single scattered wavefield data d_{syn} and observed data d_{obs} at various shot and receiver positions, the least-squares error function becomes

$$J(m) = \frac{1}{2} \sum_{ng,ns} \int_w dw \left\| d_{syn}(x_r; x_s, w) - d_{obs}(x_r; x_s, w) \right\|^2 \tag{4}$$

The gradient with respect to the model parameters in LSRTM can be calculated by using the method based on the adjoint state as following（Plessix，2006）:

$$\nabla J(m_k) = -\left\langle \lambda_k, \frac{\partial F}{\partial m_k} \right\rangle \tag{5}$$

Where F is de-migration equation. λ_k is the adjoint-state variables which can be calculated by backpropagating the residual. The update of the gradient by using the adjoint-state method (equation (5)) will suffer from low frequency artifacts, which slow down the convergence during the iterations and. In order to suppress the low-frequency noise and accelerate the convergence, we propose a linear Born inverse scattering imaging operator to efficiently update the gradient with respect to the model parameters in LSRTM as following:

$$\begin{aligned} \nabla J(m_k) = \sum_{ng,ns} \int_\omega \Big(& -\frac{\omega^2}{v_0^2(x)} \lambda_k \left[G_0(x; x_s, \omega) s(\omega) \right]^* \\ & + \nabla \left[G_0(x; x_s, \omega) s(\omega) \right]^* \cdot \nabla \lambda_k d\omega \end{aligned} \tag{6}$$

where $*$ donates the adjoint, ng and ns denote receivers and sources, respectively.

Example

We demonstrate the potential advantages of LSRTM with the inverse scattering imaging condition in comparison with the conventional zero-lag cross-correlation imaging condition of the Salt2d model. We choose the Salt2d model as it has a salt body, which causes backscattering of energy in both source and receiver wavefields. The Salt2d model is 6490 x 1700 m and generate 129 shot records with shot spacing of 50m. The maximum recording time is 3 second and a Ricker wavelet with 25Hz dominant frequency has been chosen as the source.

Figure 1(a) displays the true Salt2D velocity model. Conventional RTM and LSRTM images without any type of additional image filters after 20 iterations are shown in Figure 1(b) and Figure1(c), respectively. It can be seen from Figure 1(b) that conventional RTM suffers from low frequency artifacts problem because of the conventional crosscorrelation imaging condition is employed. In contrast, LSRTM can eliminate low frequency noise and create an image whose amplitudes are more balanced. Theoretically, LSRTM can completely recover the subsurface reflectivity model.

The linear Born inverse scattering imaging condition RTM and LSRTM images without any type of additional image filters after 20 iterations are shown in Figure 1(d) and Figure 1(e), respectively. By comparison the linear Born inverse scattering imaging condition RTM can greatly suppress low frequency artifacts than the conventional crosscorrelation imaging condition RTM. From Figure 1(d) and Figure 1(e), we can see that the linear Born inverse scattering imaging condition LSRTM creates a more balanced amplitudes image than the linear Born inverse scattering imaging condition RTM.

As we all know, LSRTM can completely recover the subsurface reflectivity model. But the conventional crosscorrelation imaging condition LSRTM eliminating low frequency noise is inefficient during the iterations because of many of the iterations are spent on removing the low frequency noise. Thus for a limited number of iterations, the iterative reflectivity image has not been effectively updated. Figure 1(c) is the conventional crosscorrelation imaging condition LSRTM result after 20 iterations. Figure 1(e) is the linear Born inverse scattering imaging condition LSRTM result after 20 iterations. Comparing Figure 1(c) with Figure 1(e), we can obviously find that the linear Born inverse scattering imaging condition LSRTM improves the imaging quality effectively, especially, sub-salt imaging quality. This is because the linear Born inverse scattering imaging condition can reduce the low frequency noise and the gradient of LSRTM calculated by the linear Born inverse scattering imaging condition is free of low

DOI:10.1190/FWI2017-028

frequency noise. The update of gradient of the linear Born inverse scattering imaging condition LSRTM is mainly used for updating reflectivity image rather than removing low frequency noise. Figure 2 is normalized residual error curve of the inverse scattering imaging condition LSRTM (ISC LSRTM) and crosscorrelation imaging condition LSRTM (CCC LSRTM). It can be seen from Figure 2 that the descent of the objective function of the inverse scattering imaging condition LSRTM is larger than that of the conventional cross-correlation imaging condition LSRTM in the first five iterations. So, updating the gradient of the objective function by the linear Born inverse scattering imaging condition is a method that can accelerate the convergence and improve the imaging quality effectively.

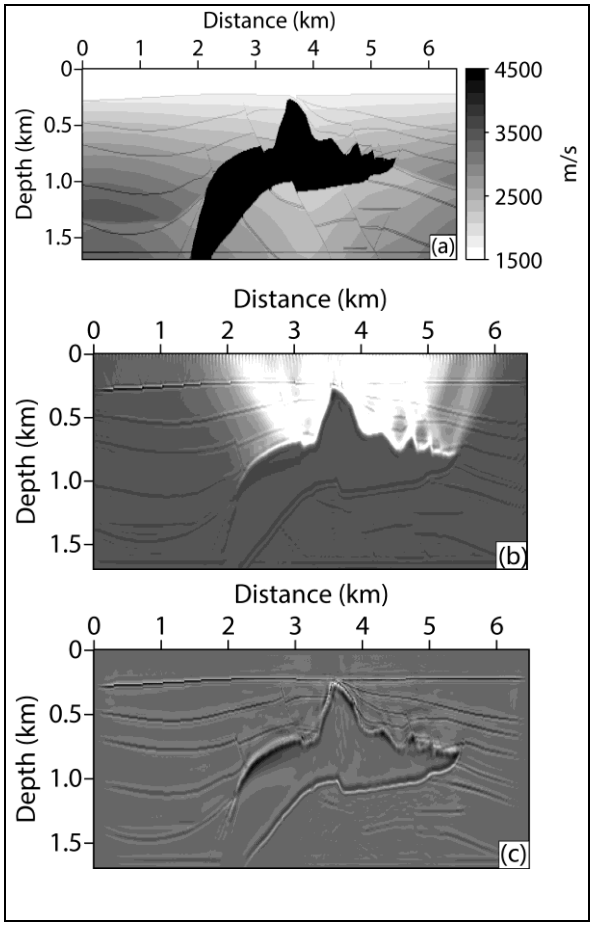

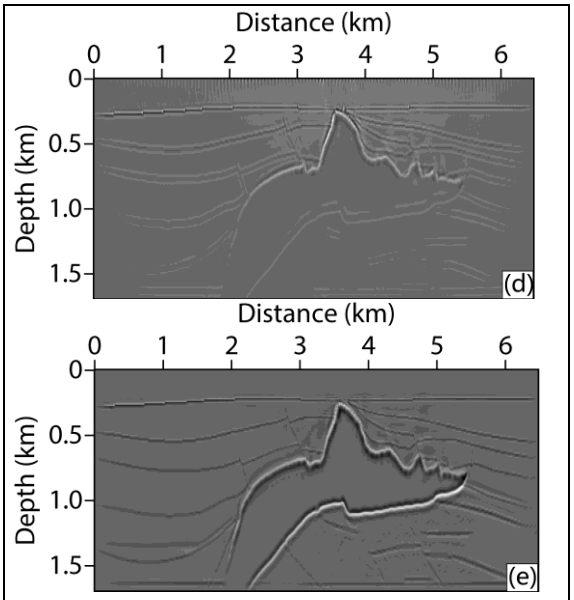

Figure 1: RTM and LSRTM with different imaging conditions

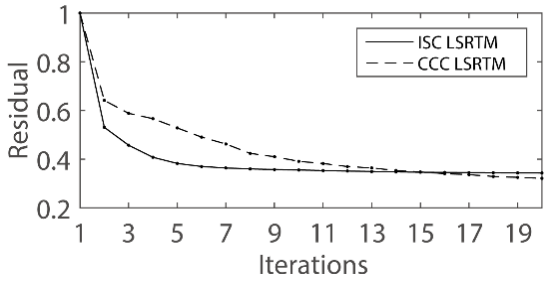

Figure 2: Normalized residual of inverse scattering imaging condition LSRTM (ISC LSRTM) and crosscorrelation imaging condition LSRTM (CCC LSRTM)

Conclusions

Although the least squares inverse time migration has the advantages of high resolution, amplitude equalization and amplitude preservation, the gradient of the objective function calculated by the adjoint-state method may suffer from low frequency artifacts which can slow down the convergence. Therefore the reflectivity model cannot be effectively updated during the iterations. The linear Born inverse scattering imaging condition is able to suppress low-frequency artifacts that appear in RTM images and LSRTM gradients. This imaging condition can efficiently update the gradient to update reflectivity image rather than to remove the low frequency noise. The numerical results show that LSRTM with the linear Born inverse scattering

DOI:10.1190/FWI2017-028

imaging condition can improve the imaging quality effectively in comparison to LSRTM with the cross-correlation imaging condition.

REFERENCES:

Baysal, E., Kosloff, D. D. and Sherwood, J.W.C., 1983, Reverse time migration. Geophysics, 48(11): 1514–1524.

Claerbout, J. F., 1971, Toward a unified theory of reflector mapping[J]. Geophysics, 36(3): 467-481.

Baysal, E., Kosloff, D. D. and Sherwood, J. W. C., 1984, A two-way nonreflecting wave equation[J]. Geophysics, 49(2): 132-141.

Loewenthal, D., Stoffa, P. L. and Faria, E. L., 1987, Suppressing the unwanted reflections of the full wave equation[J]. Geophysics, 52(7): 1007-1012.

Fletcher, R. P., Fowler, P. J., Kitchenside P., et al., 2006, Suppressing unwanted internal reflections in prestack reverse-time migration[J]. Geophysics, 71(6): E79-E82.

Yoon, K., Marfurt, K. J., 2006, Reverse-time migration using the Poynting vector[J]. Exploration Geophysics, 37(1): 102-107.

Zhang, Y., Sun, J., 2009, Practical issues in reverse time migration: true amplitude gathers, noise removal and harmonic source encoding. First break, 26: 843-852.

Liu, F. Q., Zhang, G. Q., Morton S. A., et al., 2011, An effective imaging condition for reverse-time migration using wavefield decomposition[J]. Geophysics, 76(1): S29-S39.

Op't Root, T. J., Stolk, C. C. and de Hoop, M. V., 2012, Linearized inverse scattering based on seismic reverse time migration[J]. Journal de Mathematiques Pures et Appliquees, 98(2): 211-238.

Nemeth, T., Wu, C. and Schuster, G. T., 1999, Least-squares migration of incomplete reflection data[J]. Geophysics, 64(1): 208-221.

Dai, W., Fowler, P. and Schuster, G. T., 2012, Multi-source least-squares reverse time migration[J]. Geophysical Prospecting, 60: 681-695.

Yao, G., Jakubowicz, H., 2012, Least-squares reverse-time migration[J]. SEG Technical Program Expanded Abstracts, 4609-4614.

Yao, G., Wu, D., 2015, Least-squares reverse-time migration for reflectivity imaging[J]. Sci. China Earth Sci. 58: 1982-1992.

Yao, G., Jakubowicz, H., 2016, Least-squares reverse-time migration in a matrix-based formulation[J]. Geophys. Prospect, 64: 611-621.

Plessix, R. E., 2006, A review of the adjoint-state method for computing the gradient of a functional with geophysical applications[J]. Geophysical Journal International, 167, 495-503.